



ELSEVIER

Contents lists available at ScienceDirect

Microporous and Mesoporous Materials

journal homepage: www.elsevier.com/locate/micromeso

Facile synthesis of dual micro/macroporous carbonaceous foams by templating in highly concentrated water-in-oil emulsions



Mohammad Mydul Alam^a, Jonathan Miras^a, Lourdes Adriana Pérez-Carrillo^b, Susana Vílchez^a, Conxita Solans^a, Toyoko Imae^c, Masaki Ujihara^c, Jordi Esquena^{a,*}

^a Institute for Advanced Chemistry of Catalonia, Spanish Council for Scientific Research (IQAC-CSIC) and CIBER de Bioingeniería, Biomateriales y Nanomedicina (CIBER-BBN), Jordi Girona, 18-26, 08034 Barcelona, Spain

^b Departamento de Ingeniería Química, Universidad de Guadalajara, Boul. M. García Barragán, 1451, 44300 Guadalajara, Jalisco, Mexico

^c Graduate Institute of Applied Science and Technology, National Taiwan University of Science and Technology, 43 Keelung Road, Section 4, Taipei 10607, Taiwan

ARTICLE INFO

Article history:

Received 16 January 2013

Received in revised form 8 June 2013

Accepted 12 August 2013

Available online 20 August 2013

Keywords:

Highly concentrated emulsions

Carbonaceous foams

Micro/macro dual porous materials

ABSTRACT

A simple method to synthesize carbonaceous porous foams is described, forming simultaneously micropores and macropores, by polymerizing in the external phase of highly concentrated water-in-oil (W/O) emulsions, and pyrolyzing the resulting macroporous polymer foam. Highly concentrated W/O emulsions were prepared with 1,1-dichloroethene monomer in the external phase, which was polymerized at low temperature by a redox initiator. Monolithic low-density macroporous foams were obtained after polymerization and purification by Soxhlet extraction. These foams were mainly macroporous, with low surface area ($\approx 28 \text{ m}^2 \text{ g}^{-1}$) and negligible microporosity and mesoporosity, as expected. The size (2–10 μm) and morphology of the macropores were consistent with the droplet size (2–10 μm) and shape (polyhedral) of the highly concentrated W/O emulsions. Pyrolyzation of the macroporous polymer foams allowed the formation of micropores while the macroporous texture was preserved, and consequently, dual micro/macroporous carbonaceous monoliths were obtained, with a large surface area ($> 800 \text{ m}^2 \text{ g}^{-1}$). These materials were characterized by optical microscopy, scanning and transmission electron microscopy, N_2 sorption isotherms, infrared absorption spectroscopy and elemental analysis. The influence of pyrolysis temperature (300, 400 and 500 $^\circ\text{C}$) was studied.

© 2013 Elsevier Inc. All rights reserved.

1. Introduction

Porous carbon materials are presently very important from a technological point of view. They are now extensively used as electrode materials for batteries, adsorbents, and in novel applications in supercapacitors, fuel cells, gas storage devices and supports for many catalytic processes [1–4]. The reasons for these diverse technological applications are based on some excellent physical and chemical properties, such as electrical and thermal conductivity, chemical stability, low density and wide availability. Usually, porous carbonaceous materials can be produced by pyrolysis of organic compounds, at high temperature under inert atmosphere [5]. Following methods based on this principle, porous carbon materials are prepared by carbonization of various polymers [3,6]. Moreover, complex porous textures can be obtained by using a wide variety of templates, classified into hard- or soft-templates [7]. The use of templates can allow a precise control of pore size and morphology, which is a great advantage over conventional methods for the preparation of carbon aerogels [8].

Hard templates are usually solid-state materials with well defined size and morphology, providing a rigid template for controlling porosity. Preparation of porous carbon materials has been achieved by hard-template methods based on the preparation of organic–inorganic composites, the pyrolysis of the organic polymer and the removal of the inorganic rigid scaffold, which forms the pores [9–12].

On the other hand, supramolecular self-assemblies, which are usually formed in surfactant systems, can be used as soft-templates to obtain mesoporous carbonaceous materials. In this case, the self-assembled structure is the sacrificial template, which is removed during pyrolysis [3,13].

Soft- and hard-template methods can be combined in dual templating methods, obtaining carbonaceous materials with dual porosity, that is, materials which simultaneously possess meso- and macropores [14]. These materials with dual porosities can be very efficient in catalysis and separation processes. However, the preparation methods involve several processing steps, resulting in complex and uneconomical processes. For example, the preparation of meso/macroporous carbons has been described by a multi-step method based on the use of highly concentrated emulsions [15]. A dual meso/macroporous silica material was used as

* Corresponding author. Tel.: +34 93 400 61 78; fax: +34 93 204 59 04.

E-mail address: jordi.esquena@iqac.csic.es (J. Esquena).

sacrificial template in an intermediate step. The porous structure of the silica was filled with polyfurfuryl resin, which produced carbon during pyrolyzation. Finally, the silica template was removed by dissolving in hydrofluoric acid (HF) [15].

A drawback of these methods is their complexity and time-consumption. Therefore, there is a great industrial interest in finding simple methods for the preparation of dual micro/macroporous carbonaceous low-density foams, which simultaneously possess high surface area and large pore volume. In this context, a strategy is the use of macroporous organic polymer foams, which can produce carbonaceous foams by pyrolyzation. It has been described that highly porous carbonaceous materials can be obtained by pyrolyzation of organic polymer foams, which were synthesized by polymerizing in the external phase of highly concentrated emulsions [16,17]. Different monomers could be used, such as styrene [16] or resorcinol-formaldehyde mixtures [17].

More recently, preliminary results have shown that highly concentrated emulsions, consisting of oil droplets dispersed in furfuryl alcohol (oil-in-alcohol emulsions) can be used to obtain carbonaceous low-density foams, with high surface area, by a simple method based on polymerization in the external phase of the emulsion, followed by pyrolyzation of the resulting polymer foam [18]. However, furfuryl alcohol is rather hydrophilic, leading to unstable emulsions, and consequently a precise control of the pore size can be difficult. In any case, highly concentrated emulsions can be used to prepare carbon foams with very high pore volume and large surface area, given that the polymer produces an acceptable yield on carbonization [16–18].

Highly concentrated emulsions, often designated as high internal phase emulsions (HIPEs), are characterized by having a volume fraction of the disperse phase larger than 0.74, which is the maximum packing fraction for monodispersed spherical spheres [19,20]. Because of this large volume fraction, highly concentrated emulsions consist of polyhedral and/or polydisperse droplets separated by a thin film of continuous phase [21,22]. Highly concentrated emulsions have stimulated research because of their remarkable (rheological, optical) properties, useful in practical applications such as cosmetics, foods, pharmaceuticals, aviation fuels, emulsion explosives, etc.

A very interesting application of highly concentrated emulsions is their use as templates for the preparation of low-density macroporous polymer foams. Since the first report by Bartl and Von Bonin [23] and the results of Barby and Haq [24], highly concentrated emulsions have been used to prepare a wide variety of different macroporous polymer foams [15–17,25–27]. The common strategy for the preparation of these polymeric foams is to polymerize in the continuous phase, followed by the removal of the disperse phase. The resulting materials can possess densities lower than 0.05 g mL^{-1} and total pore volumes larger than 20 mL g^{-1} , depending on the volume fraction of the emulsion-dispersed phase. As a result, a renewed interest is triggered in formulation of highly concentrated emulsions.

In the present study a simple method, based on using highly concentrated emulsions as templates, has been used for the preparation of carbonaceous foams, which simultaneously have high pore volume and large surface area. Vinylidene chloride (1,1-dichloroethene, abbreviated DCE) was used as the constituent of the oil phase because decomposes on heat treatment to produce carbon and hydrogen chloride, with an acceptable yield on carbon formation [5,28–30]. Other advantages of using DCE are the low carbonization temperature, since about 95% of the available hydrogen chloride is released on heating at $400 \text{ }^\circ\text{C}$, and the absence of large quantities of heteroatoms [28,29]. Moreover, another advantage of DCE is its high hydrophobicity and thus water-in-monomer emulsions can be much more stable than using polar monomers such as resorcinol [17] or furfuryl alcohol [18]. In addition, dis-

solved surfactants in hydrophobic monomers can form micelles. The presence of these self-aggregates, which is less favored when using polar monomers such as furfuryl alcohol, may have a beneficial effect for mesopore formation.

In the present work, water-in-DCE highly concentrated emulsions were prepared. These emulsions were characterized by optical microscopy and the polymer foams have been studied by scanning electron microscopy (SEM), transmission electron microscopy (TEM), Fourier transform infrared (FTIR) absorption spectroscopy and nitrogen sorption. The final pyrolyzed carbonaceous materials have been characterized by SEM, TEM, nitrogen sorption and elemental analysis. The thermal effects on the morphology of the carbonaceous materials have also been analyzed.

2. Experimental section

2.1. Materials

Pluronic surfactant P123 ($\text{EO}_{20}\text{-PO}_{70}\text{-EO}_{20}$, $M_w = 5750 \text{ g mol}^{-1}$) was a gift from BASF, Germany. Monomer 1,1-dichloroethene (DCE, 99 wt.%) was a product from Sigma–Aldrich. The redox initiator was a mixture of potassium persulfate ($\text{K}_2\text{S}_2\text{O}_8$, 99 wt.%) supplied by Merck and iron sulfate (FeSO_4 , 99 wt.%) by Sigma–Aldrich. Purified Milli-Q water was used for sample preparation.

2.2. Methods

2.2.1. Preparation of highly concentrated emulsions

Highly concentrated W/O emulsions, consisting of water droplets dispersed in DCE monomer, were prepared through the conventional method [31], which consists in stepwise addition of water, with vortex-mixing, to the previously prepared mixture of surfactant (P123) and oil (DCE). The surfactant/monomer weight ratio was fixed at 10/90 and the temperature was kept constant at $25 \text{ }^\circ\text{C}$. A typical final composition consists of 2 wt.% P123 surfactant, 80 wt.% H_2O and 18 wt.% DCE.

2.2.2. Polymerization of DCE in highly concentrated emulsions

Poly(1,1-dichloroethene), abbreviated as polyDCE, monoliths were prepared by polymerizing in the continuous phase of highly concentrated water-in-monomer emulsions. Polymerization was performed during 48 h at $25 \text{ }^\circ\text{C}$, lower than the boiling point of DCE monomer ($32 \text{ }^\circ\text{C}$). For the same reason, a low-temperature redox initiator was added to water, consisting of a mixture of 1.5 wt.% $\text{K}_2\text{S}_2\text{O}_8$ and 0.5 wt.% FeSO_4 (concentrations referred to the monomer).

2.2.3. Purification and pyrolysis of synthesized monoliths

The impurities (surfactant, residual monomer and initiator) were removed by soxhlet extraction with ethanol for 12 h. Afterwards, the materials were dried at room temperature until constant weight. Pyrolysis was carried out at 300, 400 or $500 \text{ }^\circ\text{C}$, in a carbolite GHA 12/450 furnace, under nitrogen atmosphere and increasing the temperature at $2 \text{ }^\circ\text{C}/\text{min}$, and keeping constant temperature for 4 hours.

2.2.4. Fourier transform infrared absorption spectroscopy

The polymerization process was confirmed by using a Nicolet 510 FTIR spectrophotometer. Spectra were collected at 4 cm^{-1} resolution with 64 averaged scans. Solid samples were ground with dried KBr and the pellets were prepared by compression in a mould.

2.2.5. Microscopy

Highly concentrated emulsions were observed by optical microscopy, in a Leica Reichert Polyvar 2 microscope. The topography of porous materials was observed by SEM, using either a JEOL JSM-6500F field emission or a HITACHI-2300 instrument. Surface treatment by sputtering was not needed for SEM observations, since the materials were already conductive. The nanostructure was observed using a Hitachi H-7000 TEM. Samples for TEM were placed on a carbon-coated copper grid, also without any further treatment.

2.2.6. Thermogravimetric analysis (TGA)

10 mg samples were introduced into platinum capsules, which were heated from 25 to 800 °C, at 10 °C/min, under N₂ atmosphere. Weight was monitored with a TGA/SDTA581 (Mettler Toledo) instrument.

2.2.7. N₂ sorption isotherms

Nitrogen adsorption and desorption isotherms were determined at 77.3 K using a Quantachrome Autosorb-iQ apparatus. The specific surface area (S_{BET}) was calculated applying the Brunauer-Emmet-Teller equation to the adsorption isotherm over the relatively low-pressure range (0.05–0.3 p/p_0). Mesoporosity was analyzed from the desorption curve of the isotherms, using two different calculation methods; Barrett-Joyner-Halenda (BJH) method was used for non-pyrolyzed materials and Non Local Density Functional Theory (NLDFT) method [32] was applied to pyrolyzed materials, since NLDFT is appropriate for microporous materials. The micropore volume (V_{micro}) and the micropore area (S_{micro}) were estimated using the t-plot equation, according to the method described by de Boer [33].

The total pore volume, V_p , which included all pores, was calculated directly from the monolith weight and volume (Eq.(1)),

$$V_p = \frac{(V_T - \frac{M}{\rho})}{M} \quad (1)$$

where V_T is the monolith volume, M is the weight and ρ is the density of non-porous carbon, assumed to be 2.0 g mL⁻¹, which is the density of graphite. This simple method was used instead of Hg porosimetry, which could damage the samples.

2.2.8. Elemental analysis

Chemical compositions (C, H and Cl) were determined using either a Flash 1112 elemental analyzer, for carbon and hydrogen contents, or a Titrando 808 instrument, for chlorine concentrations.

3. Results and discussion

3.1. Preparation and characterization of highly concentrated emulsions and polymer foams

Highly concentrated emulsions were prepared by using the conventional method that consists of stepwise addition of water, containing the initiator K₂S₂O₈ + FeSO₄, to the surfactant/monomer mixture, as described in the experimental section. Fig. 1a shows a microscopic image of the highly concentrated W/O emulsion, before polymerization. This emulsion has the typical structure of a large volume fraction of disperse phase, which exceeds the maximum close packing of spherical particles (>74 vol.%) [19–22]. The droplet size distribution seems rather polydisperse and droplet size varies from ≈2 to ≈10 μm. A film of continuous phase, which is mainly composed of DCE monomer, separates the adjacent aqueous droplets in these W/O emulsions.

Polymerization of DCE was carried out in the continuous phase of highly concentrated W/O emulsions at 25 °C, as it was described

in the experimental section. The redox initiator, dissolved into the aqueous droplets, induced polymerization by radical opening of double bonds. Afterwards, polyDCE monoliths were extracted from the moulds, and macroporous foams were obtained after washing (Soxhlet method) and drying. Fig. 1b shows the SEM image of polyDCE. The size of macropores (≈2–10 μm) is approximately the same size as the W/O emulsion droplets. Consequently, the architecture of the porous polymer foam replicates the morphology of the initial emulsion, indicating that the system was stable during polymerization, as described with other monomers [11].

The visual aspect of macroporous polyDCE monoliths is shown in Fig. 1c. Monoliths with controlled macroscopic shape (in the centimeter range) were obtained, depending on the mould, indicating that polymerization took place.

The polymerization reactions were confirmed by FTIR (Fig. 2). The spectrum shows two characteristic bands for DCE monomer at 3026 cm⁻¹ (weak peak), attributed to the =C–H stretching mode and at 1620 cm⁻¹ (sharp peak) for the C=C stretching mode (Fig. 2). These bands are not present in the spectrum of polyDCE obtained after polymerization, indicating that the reaction was almost complete. A sharp band appeared at 1356 cm⁻¹ in the polyDCE spectrum, can be attributed to CH₂ wagging mode [34]. This band associated to CH₂ groups was absent in the monomer spectrum, and it was observed only after polymerization, as expected.

From the above results, it can be concluded that the redox initiator (K₂S₂O₈ + FeSO₄) is able to polymerize at a temperature of 25 °C, facilitating the preparation of porous materials with the volatile DCE monomer.

The polymerized low-density foams were purified by soxhlet solvent extraction, with ethanol, during 12 h. It was observed that ethanol was able to penetrate rapidly inside the monoliths and the polyDCE monoliths sank, due to its higher density. This indicated that the pores were connected each other and most of air could be removed easily.

3.2. Pyrolysis of polyDCE and characterization of porous carbonaceous materials

Thermogravimetric analysis of polyDCE under N₂ atmosphere was performed from 25 to 800 °C, in order to interpret the pyrolysis process and to select the most appropriate pyrolysis temperature. The TGA data is presented in Fig. 3a.

The TGA results, as a function of pyrolysis temperature, indicate a small weight reduction up to 200 °C, probably due to the removal of moisture and solvent. A remarkable weight loss (≈50 wt.%) occurred from 200 to 300 °C, indicating the thermal decomposition of the polymer, probably by removal of HCl_(g), and leading to a carbon enriched material [5]. A further thermal decomposition (reaching a total loss around 80 wt.%) was observed at higher temperatures (between ≈300 and ≈600 °C) and the remaining weight at 800 °C was rather low, around 12 wt.%. Therefore, intermediate pyrolysis temperatures were selected, between 300 and 500 °C, under nitrogen atmosphere.

Low-density carbonaceous monoliths with an intense black color were obtained at all temperatures. The bulk density of the sample pyrolyzed at 400 °C, which retained a pristine cylindrical shape, was approximately 0.25 g mL⁻¹. The porous texture of the carbonaceous materials, treated at different pyrolysis temperatures (300 °C, 400 °C and 500 °C), is shown in Fig. 3b–d. The SEM image of the carbonaceous materials pyrolyzed at 300 °C (Fig. 3b) indicates no severe damage of the macropores structure, since the pore size distribution cannot be distinguished from that observed in the non-pyrolyzed macroporous foam (Fig. 1b).

At higher temperatures, 400 and 500 °C (Fig. 3c and d), the macropores greatly increased size (from ≈10 μm at 300 °C to >100 μm at 500 °C) and became highly polydisperse. This increase in pore

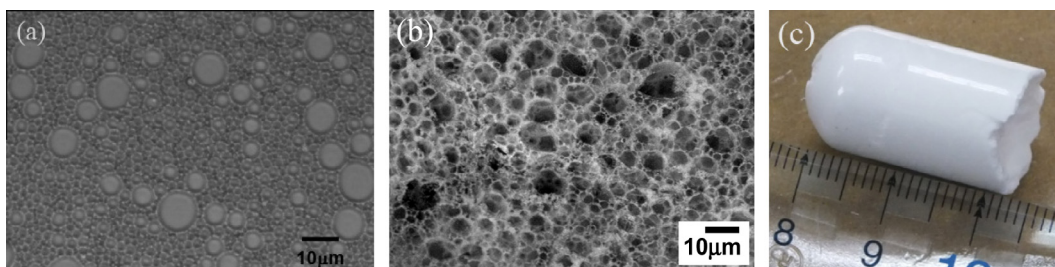


Fig. 1. (a) Morphology of highly concentrated emulsion observed by optical microscopy, (b) texture of the polyDCE foam observed by scanning electron microscopy and (c) image of the polyDCE monolith.

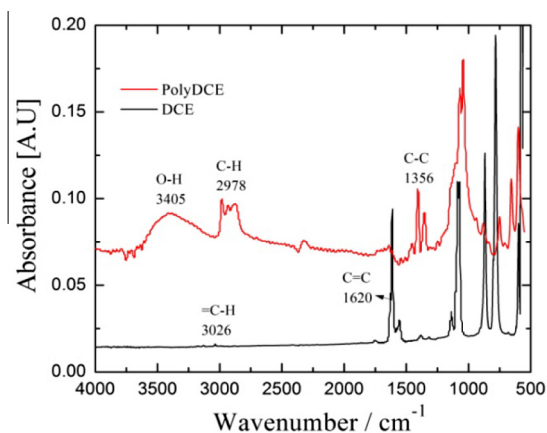


Fig. 2. FTIR absorption spectra for DCE monomer and polyDCE polymer. For clarity, the IR absorbance of polyDCE was multiplied by an arbitrary factor.

size is certainly huge (more than one order of magnitude), and it is the opposite as described by other authors, who reported that the sizes of macropores [35,36] and mesopores [37] decreased due to shrinkage during pyrolysis. The hypothesis could be that macropore size increases by pore coalescence, with rupture of pore walls. The polyDCE organic polymer is probably rather soft and deformable at high temperature (melting point ≈ 200 – 210 °C [38]). Moreover, another factor to be considered is the influence of the release of a large volume of volatile vapors during polyDCE decomposition. For example, it has been described that $\text{HCl}_{(g)}$ produced during pyrolysis could build up a high internal pressure that breaks the polymeric foam [5,29]. In any case, TGA determination (Fig. 3a) shows that carbonization is produced at approximately the same temperature (around 200 °C) and therefore it could be presumed that DCE foams do not collapse into a polymer melt because carbonization occurs simultaneously with melting.

Pyrolyzation is a rather complex process. It has been described that highly unsaturated polyene molecules are formed during pyrolysis [5,39], when $\text{HCl}_{(g)}$ is eliminated from polyDCE. These

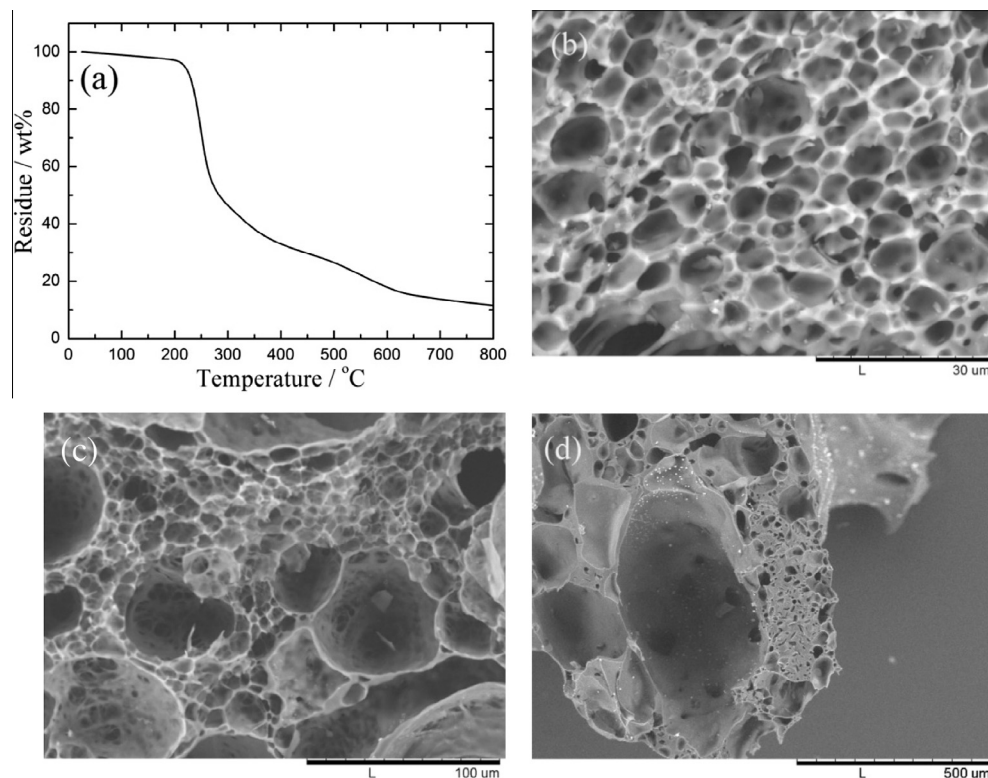


Fig. 3. (a) TGA analysis of pyrolyzed polyDCE under N_2 atmosphere; SEM micrographs of polyDCE pyrolyzed at (b) 300 °C, (c) 400 °C and (d) 500 °C.

polyenes cross-link and condense with neighboring chains, producing aromatic cores, which continue to grow edgewise and eventually form dense graphite layers [40], at temperatures around 1000 °C. In the present work, the pyrolysis temperature is lower and probably carbon remains amorphous. The samples were observed by TEM, and a disordered texture could be seen (Fig. 4).

The allotropic structure was also studied by X-ray diffraction (XRD). The typical peaks of graphite are absent in the spectrum (shown as supporting information, Fig. S1), confirming the amorphous structure of the carbonaceous materials.

3.3. N_2 isotherms of both non-pyrolyzed and pyrolyzed materials

Nitrogen isotherms were used to study the porosity of both non-pyrolyzed and pyrolyzed materials, for different temperatures (300 °C, 400 °C and 500 °C) and the data is presented in Fig. 5a. The non-pyrolyzed material shows the typical adsorption and desorption isotherms of a purely macroporous foam (type II isotherm, according to IUPAC classification) with a hysteresis loop at high relative pressure and a small adsorbed volume at low relative pressure, which indicates absence of both micropores and mesopores. The BET surface area of this non-pyrolyzed material is $28 \text{ m}^2 \text{ g}^{-1}$ with a good fit to the BET equation (0.9999 correlation coefficient).

The size distribution of the pores was calculated using BJH method (for non-pyrolyzed material) and NLDFT method (for pyrolyzed carbonaceous materials) and the data are shown in Fig. 5b. The non-pyrolyzed material showed a small volume of mesopores, confirming that this material is mainly macroporous.

The surface area greatly increased during pyrolysis from $28 \text{ m}^2 \text{ g}^{-1}$ (non-pyrolyzed) to $854 \text{ m}^2 \text{ g}^{-1}$ (pyrolyzed at 500 °C). The results on surface area, considering the total area calculated by BET method and the micropore area estimated from the t-plot [33], are presented in Table 1. The increase in surface area can be attributed to the formation of micropores, since the micropore area is rather high and similar to the total surface area. The volume of micropores is also listed in Table 1. The large micropore volume is evidenced by the huge N_2 adsorbed volume ($>50 \text{ mL g}^{-1}$, STP)

at very low pressure ($p/p_0 \approx 0.001$) (Fig. 5a) and confirmed by a good t-plot fit (Fig. 5c). The presence of micropores is not surprising, since thermal decomposition of organic polymers usually leads to the formation of microporous carbons, as it is well known in the literature [5,41].

Only the sample pyrolyzed at 300 °C may have a significant amount of mesopores, since a large hysteresis loop is observed in the isotherms and the BET surface area of this sample increases to $357 \text{ m}^2 \text{ g}^{-1}$. The hysteresis loop could be due to the existence of ink-bottle pores, with narrow necks, since the desorption branch of the isotherm is not close to the adsorption branch at low pressure, because of the obstruction by capillary condensation in the pore necks, as described by McBain [42]. In the present sample, the pores could be interconnected with a three dimensional network and a wide size distribution, producing a pore morphology similar to ink-bottle structures, and hence pore blocking could occur and a large hysteresis cycle in a wide range of relative pressure. The isotherms were not studied in more detail, at very low pressures, due to instrumental limitations and also because of the deflection from the scope of the present paper.

In any case, the adsorption isotherm resulting from the sample treated at 300 °C can be classified as a Type I isotherm, according to IUPAC, clearly indicating the existence of microporosity. The adsorbed nitrogen volume seems to reach a limiting value at the highest pressure (constant adsorption when $p/p_0 \rightarrow 1$), which is typical for activated carbons, where the maximum adsorption could be dependent on the accessibility to micropores [43].

Regarding the sample pyrolyzed at 400 °C, the adsorption isotherm showed a type I isotherm with a very small hysteresis loop between the adsorption and desorption curves. Consequently, this sample is mainly microporous, since the small loop indicates little existence of mesopores [43]. Microporosity can be the principal contribution to the total surface area, as shown in Table 1, where the area attributed to micropores is $733 \text{ m}^2 \text{ g}^{-1}$ and the overall surface is $782 \text{ m}^2 \text{ g}^{-1}$ (Table 1). Consequently, this sample has a dual micro/macroporous structure.

The total pore volume (3.5 mL g^{-1}) of the monolith obtained at 400 °C was calculated from its bulk density (0.25 g mL^{-1}), applying Eq. (1), since this monolith had a regular cylindrical shape. The value of the total pore volume is much larger than the micropore volume. Consequently, macroporosity is the main contribution to the overall pore volume, as expected, whereas microporosity is the main contribution to the surface area.

The hysteresis loop is even smaller, almost no visible within the experimental error, for the sample pyrolyzed at 500 °C. This sample also produced a clear type I adsorption isotherm, and its total surface area, $854 \text{ m}^2 \text{ g}^{-1}$, was the highest among three samples. Therefore, this sample also had a dual micro/macroporous structure, with a more evident microporous texture and negligible existence of mesopores.

3.4. Elemental analysis of non-pyrolyzed and pyrolyzed materials

For technological applications of the materials, it is necessary to control the chemical composition. The carbon content increases with the pyrolyzation temperature. However, the yield decreases, as indicated by TGA results. Fig. 3a showed that the residue was only around 12 wt.% after reaching a pyrolysis temperature of 800 °C. Therefore, the temperature should be optimized, searching for the conditions in which it is possible to obtain both acceptable carbon content and yield. The chemical compositions of the non-pyrolyzed and pyrolyzed materials were determined and compared to the theoretical value of a non-pyrolyzed sample (Table 2).

The chemical formula of the polymer is $[\text{CH}_2\text{CCl}_2]_n$, and therefore, the theoretical element composition is 24.8 wt.% C, 73.1 wt.% Cl and 2.0 wt.% H. A similar composition was found in

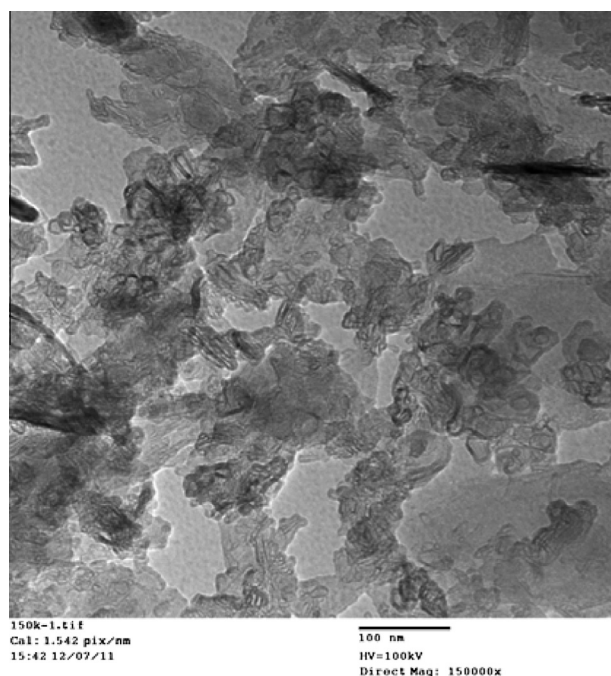


Fig. 4. Example of TEM image, obtained from the carbonaceous material treated at 400 °C. The scale bar indicates 100 nm.

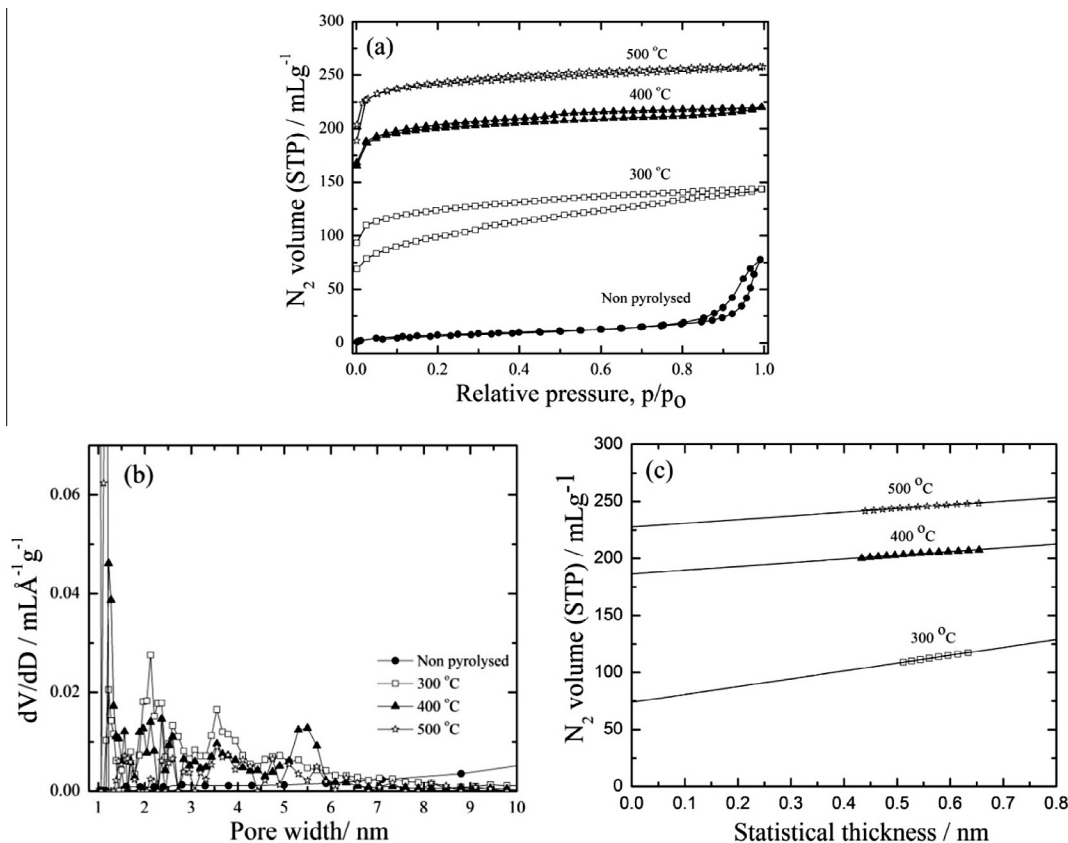


Fig. 5. (a) Nitrogen adsorption and desorption isotherms (at 77 K) of non-pyrolyzed and pyrolyzed materials, (b) pore size distributions (expressed as incremental volume per differential pore diameter dV/dD) calculated from the desorption curve by applying BJH method (for the non-pyrolyzed material) and NLDFT method (in the case of pyrolyzed samples) and (c) t-plot for the pyrolyzed materials, showing the linear fit used to estimate the volume and surface area of micropores.

Table 1

Surface area by BET method (S_{BET}) and from t-plot (S_{micro}) for the non-pyrolyzed and the pyrolyzed samples. The micropore volume (V_{micro}) obtained from the t-plot, is also shown.

Pyrolyzation temperature/°C	$S_{\text{BET}}/\text{m}^2 \text{g}^{-1}$	$S_{\text{micro}}/\text{m}^2 \text{g}^{-1}$	$V_{\text{micro}}/\text{mL g}^{-1}$
Non-pyrolyzed	28	≈0	≈0
300	357	252	0.11
400	782	733	0.29
500	854	804	0.35

Table 2

Elemental analyses of the non-pyrolyzed and pyrolyzed materials.

Pyrolyzation temperature/°C		C/wt.%	Cl/wt.%	H/wt.%	C/H molar ratio
Non-pyrolyzed	Theoretical	24.8	73.1	2.1	1/1
	Experimental	26.4	65.7	2.4	0.9/1
Pyrolyzed	300 °C	60.7	23	1.4	3.6/1
	400 °C	62.2	20	1.5	3.5/1
	500 °C	75.9	8.5	1.1	5.8/1

the experimental non-pyrolyzed sample (26.4/65.7/2.4 mass ratios) but with a slightly smaller chlorine content, which could be due to monomer impurities.

Table 2 clearly reveals that carbon content greatly increased with pyrolyzation, from 26.4 wt.% (non-pyrolyzed sample) to 75.9 wt.% (sample pyrolyzed at 500 °C). Consequently, the C/H molar ratio increased from the theoretical value of 1/1 to 5.8/1 at 500 °C, and therefore the materials were greatly enriched in carbon. Regarding chlorine content, it decreased down to 8.5 wt.% at

500 °C. These values are similar to those already described by Marsh and Wynne-Jones [28], who pyrolyzed poly(1,1-dichloroethene) by increasing temperature at 5 °C/min rate and maintaining the final temperature for 10 h.

Some impurities could be present in the sample, since low-intensity peaks in the XRD spectrum (Fig. S1, supporting information) were observed. These peaks were consistent with KCl, which could form during pyrolyzation. It is widely known that the use of K_2SO_8 as initiator leads to formation of $[\text{CH}_2\text{CCl}_2]_n^- \text{SO}_4^- \text{K}^+$ sulfate terminal groups, covalently linked to the polymer after double bond opening, propagation of radicals and polymerization. Therefore, the pyrolyzation of such terminal groups would produce KCl. However, Fe, K and S (all from the redox initiator) were not detected in any sample by elemental analysis, and consequently, the concentration of impurities is probably low. In any case, a micro/macroporous carbonaceous material with large surface area ($854 \text{ m}^2 \text{g}^{-1}$) and high carbon content ($\approx 76 \text{ wt.}\%$) was obtained, which could be useful in many industrial applications such as separation and catalytic processes.

4. Conclusions

A facile method for the preparation of dual micro/macroporous carbonaceous foams has been developed, by polymerizing in the external phase of highly concentrated emulsions and carbonizing the macroporous polymer foam. The non-pyrolyzed polymer foam was essentially macroporous with a low surface area ($\approx 28 \text{ m}^2 \text{g}^{-1}$). The size of the macropores was very similar to the size of the emulsion droplets, which were used as templates. Carbonization of the macroporous foams was carried out by thermal treatment under

nitrogen atmosphere between 300 and 500 °C. The polymeric foam pyrolyzed at low temperature (300 °C) possessed a macropore structure similar to the non-pyrolyzed monoliths. However, macropore size greatly increased after pyrolyzation at higher temperature, along with presence of very large pores (>100 μm) probably due to pore coalescence. Pyrolyzation also induced the formation of micropores, which were produced by the thermal decomposition of the organic polymer. As a result, surface area greatly increased up to around 850 m² g⁻¹ at 500 °C. Elemental analysis indicated that the carbon content increased as a function of temperature, as expected. Relatively large carbon content, up to ≈76 wt.%, was obtained at 500 °C with a C/H molar ratio of 5.8. The procedure described in the work has indicated that the pyrolysis of macroporous foams is a simple method for the preparation of dual micro/macroporous carbonaceous low-density materials.

Acknowledgements

The authors are grateful to financial support from the Spanish Ministry of Economy and Competitiveness (CTQ2008-06892-C03-01 and CTQ2011-2348 projects). The Spanish Council for Scientific Research (CSIC) and Taiwan National Science Council (NSC) are acknowledged (2009TW0031 and NSC 99-2923-M-011-001-MY3 grants, respectively) for the joint Formosa project. M.M. Alam is also grateful to CSIC for the SB2010-0148 grant. The authors also acknowledge J.M Díez-Tascón for useful discussions.

Appendix A. Supplementary data

Supplementary data associated with this article can be found, in the online version, at <http://dx.doi.org/10.1016/j.micromeso.2013.08.015>.

References

- [1] H. Marsh, E.A. Heintz, F. Rodríguez-Reinoso, *Introduction to Carbon Technology*, Universidad de Alicante, Secretariado de Pub, Alicante, Spain, 1997. pp. 35–101.
- [2] S. Subramoney, *Adv. Mater.* 10 (1998) 1157–1171.
- [3] J. Lee, J. Kim, T. Hyeon, *Adv. Mater.* 18 (2006) 2073–2094.
- [4] A.G. Pandolfo, A.F. Hollenkamp, *J. Power Sources* 157 (2006) 11–27.
- [5] R.E. Franklin, *Proc. R. Soc.* 209 (1951) 196.
- [6] A. Oya, S. Yoshida, J. Alcaniz-Monge, A. Linares-Soleno, *Carbon* 33 (1995) 1085–1090.
- [7] C. Liang, Z. Li, S. Dai, *Angew. Chem. Int. Ed.* 47 (2008) 3696–3717.
- [8] J.W. Patrick, A. Walker, in: J.W. Patrick (Ed.), *Porosity in Carbons*, Edward Arnold, London, 1995.
- [9] T. Kyotani, T. Nagai, S. Inoue, A. Tomita, *Chem. Mater.* 9 (1997) 609–615.
- [10] R. Ryoo, S.H. Joo, S. Jun, *J. Phys. Chem. B* 103 (1999) 7743–7746.
- [11] R. Ryoo, S.H. Joo, M. Kruk, M. Jaroniec, *Adv. Mater.* 13 (2001) 677–681.
- [12] A.J.G. Zarbin, R. Bertholdo, M.A.C. Oliveira, *Carbon* 40 (2002) 2413–2422.
- [13] T.Y. Ma, L. Liu, Z.Y. Yuan, *Chem. Soc. Rev.* 42 (2013) 3977–4003.
- [14] Z. Wang, E.R. Kiesel, A. Stein, *J. Mater. Chem.* 18 (2008) 2194–2200.
- [15] S. Alvarez, A.B. Fuertes, J. Esquena, C. Solans, *Adv. Eng. Mater.* 6 (2004) 897–899.
- [16] D. Wang, N.L. Smith, P.M. Budd, *Polym. Int.* 54 (2005) 297–303.
- [17] A.F. Gross, A.P. Nowak, *Langmuir* 26 (2010) 11378–11383.
- [18] S. Vílchez, L.A. Pérez-Carrillo, J. Miras, C. Solans, J. Esquena, *Langmuir* 28 (2012) 7614–7621.
- [19] K.J. Lissant, *J. Colloid Interface Sci.* 22 (1966) 462–468.
- [20] H.M. Princen, *J. Colloid Interface Sci.* 91 (1983) 160–175.
- [21] H. Kunieda, D.F. Evans, C. Solans, M. Yoshida, *Colloids Surf. A* 47 (1990) 35–43.
- [22] C. Solans, R. Pons, S. Zhu, H.T. Davies, D.F. Evans, K. Nakamura, H. Kunieda, *Langmuir* 9 (1993) 1479–1482.
- [23] Von H. Bartl, W. Von Bonin, *Die Makromolekulare Chemie* 57 (1962) 74–95.
- [24] D. Barby, Z. Haq, Low density porous cross-linked polymeric materials and their preparation, European patent 0060138, 1982.
- [25] J.M. Williams, D.A. Wroblewski, *Langmuir* 4 (1988) 562–656.
- [26] E. Ruckenstein, J.S. Park, *J. Polym. Sci. Polym. Lett.* 26 (1988) 529–536.
- [27] P. Hainey, I.M. Huxham, B. Rowatt, D.C. Sherrington, L. Tetley, *Macromolecules* 24 (1991) 117–121.
- [28] H. Marsh, W.F.K. Wynne-Jones, *Carbon* 1 (1964) 269–279.
- [29] E.H. Boulton, H.G. Campbell, H. Marsh, *Carbon* 7 (1969) 700–701.
- [30] D.H. Davies, D.H. Everett, D.J. Taylor, *Trans. Faraday Soc.* 67 (1971) 382–401.
- [31] H. Kunieda, C. Solans, N. Shida, J.L. Parra, *Colloids Surf. A* 24 (1987) 225.
- [32] P.I. Ravikovitch, A.V. Neimark, *Colloids Surf. A* 187–188 (2001) 11–21.
- [33] J.H. de Boer, B.C. Lippens, B.G. Linsen, J.C.P. Broekhoff, A. Heuvel, Th.J. Osinga, *J. Colloid Interface Sci.* 21 (1966) 405–414.
- [34] S. Narita, S. Ichinohe, S. Enomoto, *J. Polym. Sci.* 37 (1959) 251–261.
- [35] L.Y. Xu, Z.G. Shi, Y. Feng, *Micropor. Mesopor. Mater.* 115 (2008) 618–623.
- [36] G. Hasegawa, K. Kanamori, K. Nakanishi, T. Hanada, *Carbon* 48 (2010) 1757–1766.
- [37] Y. Meng, D. Gu, F. Zhang, Y. Shi, H. Yang, Z. Li, C. Yu, B. Tu, D. Zhao, *Angew. Chem. Int. Ed.* 44 (2005) 7053–7059.
- [38] D.S. Gibbs, R.A. Wessling, B.E. Obi, P.T. DeLassus, B.A. Howell, Vinylidene Chloride monomer and polymer, *Encyclopedia of Chemical Technology*, Kirk-Othmer, 4th ed. 24, 1997, 882–923.
- [39] R.E. Franklin, *Acta Crystallogr.* 3 (1950) 107–121.
- [40] C.R. Kinney, R.C. Nunn, P.L. Walker, *Ind. Eng. Chem.* 49 (1957) 880–884.
- [41] T. Kyotani, *Carbon* 28 (2000) 269–286.
- [42] J.W. McBain, *J. Am. Chem. Soc.* 57 (1935) 699–700.
- [43] S. Lowell, E.S. Joan, M.A. Thomas, M. Thomas, *Characterization of Porous Solids and Powders: Surface Area, Pore Size and Density*, 1st ed., Springer, Amsterdam, 2004.